0026-895X/89/040458-11$02.00/0

MOLECULAR PHARMACOLOGY, 35:458-468

Aminopyridines Enhance Opening of Calcium-Activated Potassium Channels in GH_3 Anterior Pituitary Cells

MICHAEL A. ROGAWSKI

Medical Neurology Branch, National Institute of Neurological Disorders and Stroke, National Institutes of Health, Bethesda, Maryland 20892

Received October 21, 1988; Accepted January 4, 1989

SUMMARY

The effects of aminopyridine analogs on Ca^{2+}-activated K^+ channels in GH_3 clonal anterior pituitary cells were studied using whole-cell voltage-clamp and single-channel recording techniques. Step depolarization from a holding potential of −50 mV activated a noninactivating, tetraethylammonium- and Cd^{2+}-sensitive outward current. Tail current analysis indicated that this sustained outward current is carried predominantly by K^+ ions. Extracellular perfusion with 4-aminopyridine and 3,4-diaminopyridine (0.05–5 mM) caused a dose-dependent enhancement of the outward current by up to 100 and 170%, respectively. This effect typically occurred with prolonged depolarizations of >1–2 sec. Patch-clamp recordings in the cell-attached configuration demonstrated that 4-aminopyridine (2 mM) promotes the activity of a large-conductance (150–175 pS; 50–135 mM external K^+), tetraethylammonium-sensitive, Ca^{2+}-activated K^+ channel; the drug had no effect on these channels in excised patches. These results indicate that aminopyridines enhance the opening of Ca^{2+}-activated K^+ channels in GH_3 cells. Several lines of evidence suggest that this effect may occur indirectly, possibly as a result of an increase in the effective intracellular free Ca^{2+} level.

The aminopyridines are powerful convulsant agents that specifically block voltage-dependent K^+ channels in neural and muscle membranes, facilitate neurotransmitter release at peripheral and central synapses (1), and enhance hormone release from endocrine cells (2). Early studies indicated that these drugs inhibited the delayed rectifier K^+ conductance (I_K) in axons (3–5) and skeletal muscle fibers (6, 7). Later it was recognized that, in neural somata and some axons, aminopyridines are relatively selective blockers of the A-current (I_A), a low voltage-activated, rapidly inactivating K^+ current (8; see Ref. 9 for additional references). In contrast to these inhibitory effects on I_K and I_A, it has been reported that 4-AP promotes the Ca^{2+}-activated K^+ conductance in molluscan pacemaker neurons (10).

In the present study, I examined the effects of aminopyridines on Ca^{2+}-activated K^+ currents and single Ca^{2+}-activated K^+ channels in GH_3 clonal anterior pituitary cells. Previous voltage-clamp studies have demonstrated that GH_3 cells possess two major K^+ currents, a fast inactivating current similar to I_A in neural and muscle cells and a noninactivating, Ca^{2+}-dependent current [$I_{K(Ca)}$] (11–16). This noninactivating current is predominantly due to a large conductance Ca^{2+}- and voltage-dependent K^+ channel, although smaller conductance channels may also make a quantitatively small (<18%) contribution to the net current (14, 17). I recently reported that aminopyridines cause a selective blockade of I_A in GH_3 cells (15) and incidentally noted that Ca^{2+}-inactivated K^+ currents were potentiated by the drugs. The present study examines this latter observation in more detail.

Materials and Methods

Cell culture. GH_3 cells (subclone B6 of A. Tixier-Vidal and D. Gourdji, generously provided by B. Dufy, University of Bordeaux II, Bordeaux, France) were grown in 35-mm polystyrene Petri dishes as described previously (15). The cells were used for electrophysiological experiments after 2–10 days in culture. Recordings were carried out at room temperature.

Whole-cell voltage-clamp recording. Immediately before each experiment, the culture medium was replaced with Hank's balanced salt solution (GIBCO, Grand Island, NY) containing (in mM): NaCl, 137; KCl, 5.5; KH_2PO_4, 0.40; Na_2HPO_4, 0.34; HEPES, 10; $CaCl_2$, 5; $MgCl_2$, 1; and sufficient glucose to bring the osmolality to 280–310 mOsm/kg of H_2O (pH 7.40). In high K^+ solutions, the concentration of KCl was increased and the NaCl was correspondingly decreased to maintain the osmolality. Patch-clamp recording electrodes were prepared from 1.5-mm o.d. thin wall, filament-fused, borosilicate capillaries (Kwik-Fil TW150F; WPI Instruments, New Haven, CT). The electrodes were filled with a solution containing (in mM): KCl, 140; $MgCl_2$, 1; EGTA, 1.1, HEPES, 10; and sufficient glucose to obtain an osmolality of 280–310 mOsm/kg of H_2O (pH 7.40). Electrode tip resistances were typically 1.8–2.5 MΩ. Whole-cell voltage-clamp recording was carried out using a Dagan 8900 Patch Clamp/Whole Cell Clamp amplifier with a 100-MΩ headstage feedback resistor. Seal resistances were typically 10 GΩ or greater.

In some whole-cell recording experiments, the following special recording solutions were used (in mM). 1) NMG-MSA/K-MSA: *bath*,

ABBREVIATIONS: 4-AP, 4-aminopyridine; 3,4-DAP, 3,4-diaminopyridine; NMG, *N*-methyl-D-glucamine; MSA, methanesulfonic acid; TEA, tetraethylammonium; EGTA, ethylene glycol *bis*(β-aminoethyl ether)*N,N'*-tetraacetic acid; HEPES, 4-(2-hydroxyethyl)-1-piperazineethanesulfonic acid.

NMG methanesulfonate (prepared by titrating NMG with methanesulfonic acid MSA), 140; potassium methanesulfonate (prepared by titrating KOH with MSA), 5; calcium acetate, 5; $MgSO_4$, 1; HEPES, 10; and glucose to adjust osmolality to 327 mOsm/kg (in some cases 0.2 mM $CdCl_2$ was added); *electrode*, potassium methanesulfonate, 140; $MgSO_4$, 1; EGTA, 1.1; HEPES, 10; and glucose to 315 mOsm/kg (electrode resistances with this combination were approximately 4 MΩ). 2) NaCl-TEA/CsCl: *bath*, NaCl, 120; TEA, 20; KCl, 5; $CaCl_2$, 5; $MgCl_2$, 1; HEPES, 10; and glucose to 310 mOsm/kg; *electrode*, CsCl, 140; $MgCl_2$, 1; HEPES, 10; EGTA, 1.1; and glucose to 310 mOsm/kg. 3) NMG-Cl/NMG-Cl: *bath*, NMG-Cl (prepared by titrating NMG with HCl), 140; $CaCl_2$, 5; $MgCl_2$, 1; HEPES, 10; and glucose to 301 mOsm/kg; *electrode*, NMG-Cl, 140; $MgCl_2$, 1; EGTA, 1.1; HEPES, 10; and glucose to 304 mOsm/kg. All solutions were adjusted to pH 7.40. NMG and MSA were obtained from Sigma Chemical Co. (St. Louis, MO). Solutions were filtered through a 0.22-μm membrane filter (Millipore Corp., Bedford, MA) immediately before use.

Single-channel recording. Single-channel recordings were carried out in the cell-attached, inside-out, and outside-out configurations using patch electrodes prepared as described above. In this application, the 10-GΩ headstage feedback resistor was used. For cell-attached and inside-out recordings, the patch electrodes were filled with the standard bathing medium except that, in some inside-out recordings, 10 mM $CaCl_2$ and 2 mM $MgCl_2$ was used, because this aided in maintaining the integrity of the patches. Where specified, the K^+ concentration of the pipette solution was elevated with a corresponding decrease in Na^+. The bathing solution in the inside-out experiments usually contained (in mM): KCl, 140; HEPES, 10; EGTA, 1.1; $CaCl_2$, 0.1; $MgCl_2$, 1 (nominally 10^{-8} M free Ca^{2+}). For high Ca^{2+} solutions (nominally 10^{-6} M free Ca^{2}), 1 mM $CaCl_2$ was used. Recordings in the outside-out configuration used electrodes filled with the same internal solution as for whole-cell recording, except as noted in the figure legends.

Application of ions and drugs. 4-AP and 3,4-DAP were applied by pressure ejection (typically <1 p.s.i.) from glass micropipettes (prepared from 1.2-mm o.d. capillaries; tip diameter, 1–2 μm) positioned close to the cell membrane or the tip of the electrode containing an excised membrane patch. The drugs were dissolved in bathing medium and the solution was adjusted to pH 7.40 as required. Concentrations given are those in the pressure pipette. In inside-out patch experiments, changes in internal (bath) ionic concentration were accomplished by rapid perfusion. 4-AP was obtained from ICN Pharmaceuticals (Plainview, NY); 3,4-DAP and TEA were from Sigma Chemical Co.

Data acquisition and analysis. Macroscopic and single-channel membrane currents were recorded on a Brush oscillographic recorder (Gould Inc., Cleveland, OH). Single-channel currents, filtered at 1 KHz, were also acquired on a minicomputer in records of 2048 points each at a rate of 200 μsec/point and were stored on a magnetic disk for later analysis. Single-channel parameters were determined semiautomatically by manually positioning a cursor on a video display of the raw data. Curve fitting and plotting were performed with the Grapher software package (Golden Software, Golden, CO).

In all data figures, outward currents are positive (upward) and represent movement of positive charge from the cell interior to the cell exterior or, in excised patch recordings, from the internal (cytoplasmic) membrane face to the external (extracellular) membrane face.

Results

Characteristics of the sustained outward current. Depolarizing voltage-clamp steps from a holding potential of −50 or −40 mV activated an outward current that rose to an initial plateau within 200 msec. As in the recording shown in Fig. 1, upon depolarization to −25 mV or more positive potentials, the current typically exhibited a dramatic sigmoidal rise in amplitude after 0.4–2 sec of maintained depolarization. The current did not show time-dependent inactivation even when the membrane was depolarized for >5–10 sec. In a few cells, the delayed

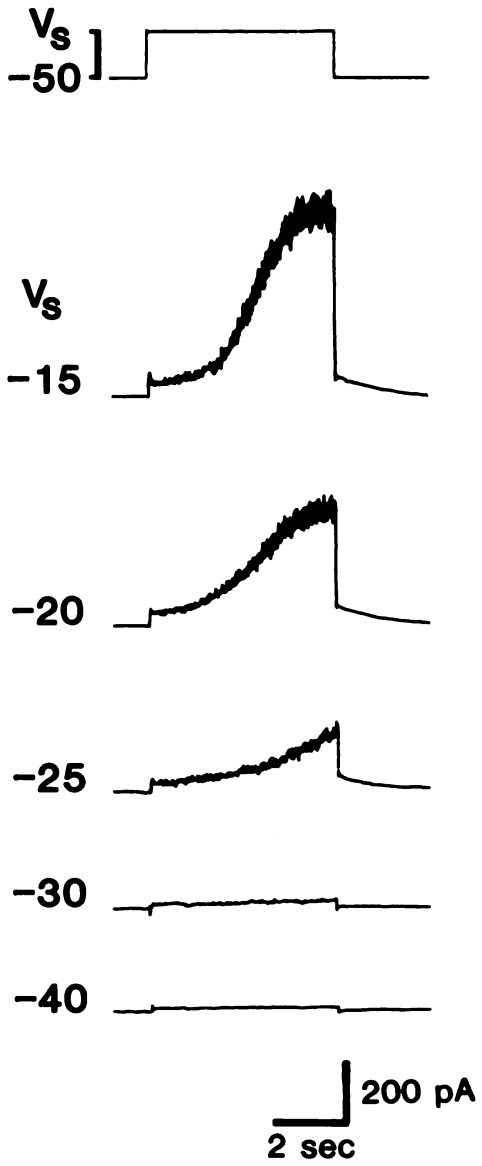

Fig. 1. Whole-cell voltage-clamp recording from a GH_3 cell showing voltage dependency for activation of the sustained outward current. The cell was held at −50 mV and stepped to the potentials (V_s) given to the *left* of each *trace*. In this and subsequent figures, all potentials are in mV and the standard bath and pipette solutions were used (see Materials and Methods) unless otherwise noted.

increase in the current diminished with repeated depolarizing steps, but in most cells the current was stable as long as the recording could be maintained (up to 30 min). As in the traces of Fig. 1, the current noise increased progressively during the slow turning on of the outward current, suggesting that the current is due to increased membrane conductance resulting from channel openings.

At a holding potential of −50 mV, the fast inactivating outward current in GH_3 cells, I_A, shows nearly complete (~90%) steady state inactivation (15). Moreover, because the bulk of this current undergoes exponential time-dependent inactivation with a time constant of 30–50 msec, the contribution of I_A to the total outward current at the end of prolonged (3–5 sec) voltage steps, as used in the present study, is insignificant.

The ionic selectivity of the sustained outward current was determined by analysis of the tail currents obtained on repo-

larization to different potentials. Under ordinary ionic conditions with 5-sec depolarizing voltage steps, the tail current observed on repolarization to −50 mV was outward and reached 1/*e* amplitude in 0.8–4.8 sec (mean ± SD: 2.3 ± 1.2; 19 cells). The decay rate was independent of step potential. Fig. 2 shows the tail currents obtained after a 5-sec depolarizing step from −50 to −20 mV under conditions of normal (5.5 mM) and elevated (10.5 mM) extracellular K^+. The reversal potential shifts from −67 to −52 mV, a 15-mV change that is near the 16-mV shift expected of a pure K^+ current at room temperature. Thus, the outward current is primarily mediated by K^+ ions. In two additional cells, the tail current reversal potentials in ordinary extracellular K^+ were −72 and −73 mV, giving a mean ± SD of −71 ± 3 mV for the three cells. There is a significant divergence of the measured reversal potentials from the values predicted by the Nernst relationship. Assuming complete replacement of the intracellular electrolyte with the pipette solution, the calculated equilibrium potential for K^+ in 5.5 mM external solution is −82 mV. The −11-mV deviation of this value from the measured tail current reversal potential is likely due to K^+ accumulation near the external membrane face during the prolonged depolarizing steps and possibly also due to contamination by Ca^{2+}-dependent Cl^- currents (18). In addition, there may be errors caused by the liquid-junction potential between the bath and pipette solutions and the Donnan potential at the electrode tip (see Ref. 14).

To confirm that the tail current reflects deactivation of the sustained outward current, a comparison was made between the outward current activated during voltage steps and the corresponding tail current for depolarizations of various durations. As illustrated in Fig. 3, the magnitude of the peak outward current and the tail current increase in parallel as the duration of the voltage step becomes longer. In the cell shown, the peak and tail currents both reached a maximum of 6 sec. Moreover, there is a close linear correlation between the outward current and tail current conductances of each step. The tail current conductance is smaller in magnitude than the peak conductance, presumably because a portion of the outward current deactivates nearly instantaneously on repolarization. These results indicate that the tail current reflects deactivation of the outward current during the step and provides support for the conclusion, based upon the reversal potential measurements, that the outward current is due to current flow through primarily K^+-selective channels.

Blockade of the sustained outward current. The sustained outward current activated by prolonged depolarization from a holding potential of −50 mV was substantially blocked by TEA and Cd^{2+}. This is ullustrated in Fig. 4, which shows current-voltage plots before and during superfusion with 25 mM TEA and 0.2 mM Cd^{2+}. Note in the sample records that these channel-blocking agents reduced both the outward current elicited during the depolarizing step and the outward tail current reflecting deactivation of this current. For the cell shown, TEA produced an 88% block of the leak-subtracted peak current at −20 mV and this block diminished to 76% at 0 mV. Cd^{2+} caused a similar degree of block as did TEA; however, in contrast to TEA, there was no voltage-dependent relief of the block as the cell was depolarized. Thus, Cd^{2+} caused an 88% block of the leak-subtracted outward current at −20 mV and a 90% block at 0 mV. The voltage dependency of the TEA effect is compatible with a channel-blocking mechanism in which the positively charged molecule plugs the channel pore. As the cell is depolarized, the electrostatic field sensed by the TEA molecule would tend to oppose binding to its acceptor site within the channel. TEA block of Ca^{2+}-activated K^+ channels in other cell types shows varying degrees of voltage dependence (19–22), indicating that TEA penetrates into the channel pore to different extents in various preparations. In contrast to the TEA block, the Cd^{2+} block likely results from an indirect mechanism, in which Ca^{2+} entry through voltage-dependent Ca^{2+} channels is prevented and intracellular Ca^{2+} levels fail to rise so that Ca^{2+}-dependent facilitation of channel opening is prevented. At 0.2 mM, Cd^{2+} has previously been shown to produce complete block of the Ca^{2+} currents in GH_3 cells (23). These pharmacological observations support the conclusion that the sustained outward current activated by prolonged depolarizing voltage-clamp steps is due primarily to activation of a Ca^{2+}-dependent K^+ conductance.

Facilitation of outward current by aminopyridines. As illustrated in Fig. 5A, 4-AP and 3,4-DAP caused a marked increase in the amplitude of the sustained outward current. The bulk of this effect is observed during the rapid rise in

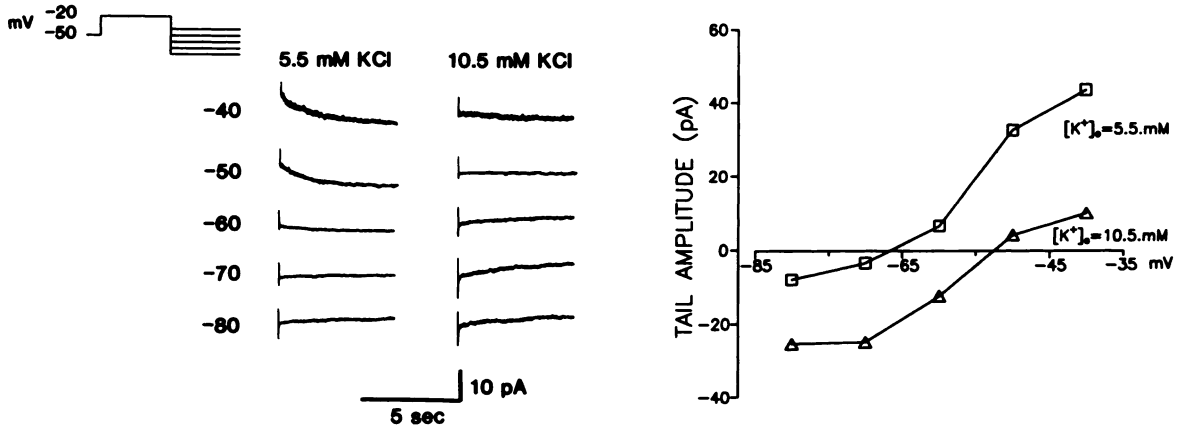

Fig. 2. Sensitivity of tail currents to a change in external K^+. Outward current was activated by a 5-sec depolarization to −20 mV from a holding potential of −50 mV. Sample records of the tail currents obtained on repolarization to various potential levels are illustrated. The amplitude of the tail current 100 msec after repolarization (measured with respect to the leakage current 6 sec after repolarization) is plotted in the graph shown to the *right*.

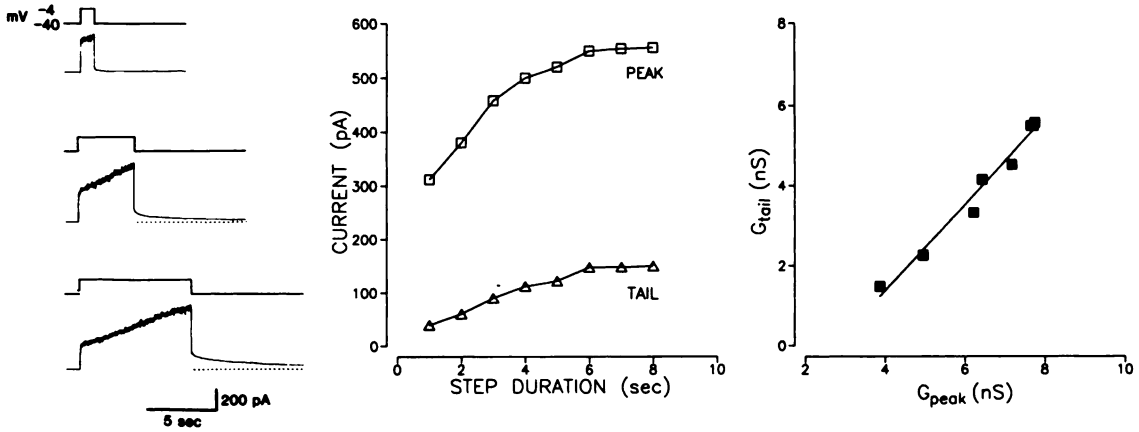

Fig. 3. Comparison of peak outward current and tail current elicited by step depoarlization from −40 to −4 mV for various durations. Sample records are shown to the *left*. The peak outward current and tail current amplitudes are plotted in the graph shown in the *middle*. The conductance of the peak current (G_{peak}) and tail current G_{tail}) was estimated by dividing the amplitude by $V-V_r$ where V is the potential at which the current was recorded and V_r is the reversal potential of tail currents in these cells (−71 mV; see text). G_{tail} is plotted against G_{peak} at the *right*; the *line* indicates the least squares fit to the data (slope, 1.08).

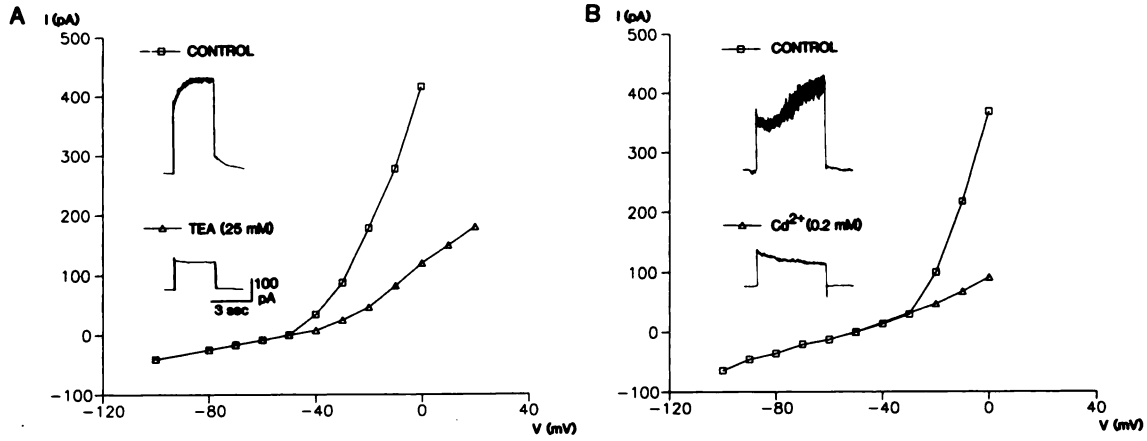

Fig. 4. Current-voltage relationships for outward current before (□) and after (△) the application of TEA (25 mM) (A) and Cd^{2+} (0.2 mM) (B). The *points* represent the peak outward current at the end of 3- (TEA) or 5- (Cd^{2+}) sec voltage-clamp steps from a holding potential of −50 mV. The *inset* shows sample records obtained with steps to 0 mV; the scale shown in (A) also applies to the records in (B).

outward current that occurs 1–3 sec after the onset of the voltage step. The facilitation of outward current begins within seconds after onset of the drug superfusion and reaches a plateau in about 1 min (Fig. 6). The effects of 4-AP and 3,4-DAP were fully reversible, so that the current typically returned to baseline levels within 30–60 sec after discontinuation of the drug superfusion (Fig. 5A). In some cells, the increase in current induced by the drugs became less prominent with repeated depolarizing voltage steps, although in two cells the enhanced current was maintained for up to 3 min after onset of the drug superfusion. As seen in the records of Fig. 5A, the outward tail current following repolarization is also increased by the aminopyridines. Fig. 6 plots the tail current conductance as the response to 4-AP develops. In comparison with the effect on the increase in the peak conductance during the step, there is a corresponding, although smaller, increase in the tail current conductance. The increase in the outward tail current is as expected if the aminopyridine facilitation of outward current is due to an increase in the activity of the K^+ channels that contribute to the sustained outward current. The dissociation between the magnitude of the increase in outward current during the step and the tail current was seen in all cells examined and may reflect enhancement by the aminopyridines of an opposing inward tail current resulting from deactivation of a Ca^{2+}-dependent Cl^- current (18). Alternatively, 4-AP may additionally enhance a rapidly deactivating outward current, the decay of which is too fast to be resolved on the time scale used in these experiments. Ritchie (14) previously observed such a partially Ca^{2+}-dependent current (deactivation time constant, ~44 msec) in a small proportion of GH_3 cells.

To confirm that the effects of 4-AP on outward current were due to promotion of K^+ channels, recordings were carried out under conditions in which K^+ was the sole membrane-permeant intracellular cation and Ca^{2+} was the only permeant extracellular cation (Fig. 5B). Under these conditions, 4-AP produced a large (683 ± 83%, mean ± SE; five cells) facilitation of outward current confirming that the effect of the drug is specifically due to an increase in K^+ conductance. (Control outward current amplitudes were smaller than those obtained with ordinary recording solutions, typically 40–175 pA with voltage steps to −10 or 0 mV, and outward tail currents were not observed under these conditions, possibly as a result of a shift in the K^+ equilibrium potential or a change in the deactivation kinetics of the current.) Addition of Cd^{2+} (0.2 mM) to the NMG-MSA extracellular mediun in recordings with K-MSA-filled pipettes eliminated the sustained outward cur-

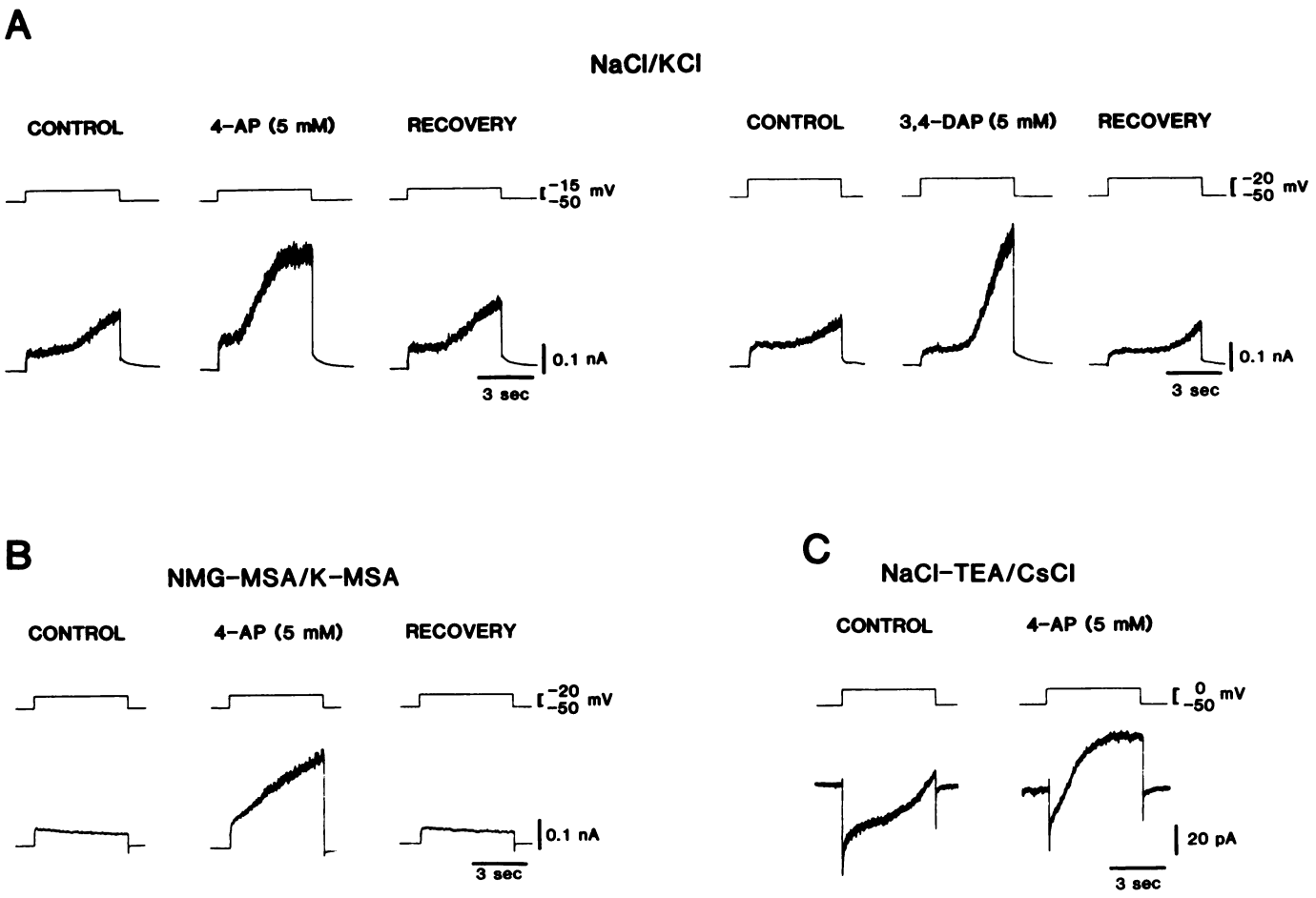

Fig. 5. Facilitation of sustained outward current by aminopyridines under different ionic conditions. A, Comparison of the effect of 4-AP and 3,4-DAP on two different cells in normal recording conditions. B, Effect of 4-AP on outward current in NMG-MSA/K-MSA (see Materials and Methods), where the sole permeant cations are Ca^{2+} (outside) and K^+ (inside). C, Effect of 4-AP on inward and outward currents in NaCl-TEA/CsCl, where K^+ channels are substantially blocked by TEA and Cs^+.

rent and, under these conditions, 4-AP failed to have any effect on the current record (three cells). Taken together, these results indicate that the ability of 4-AP to promote outward current is due to its effect on Ca^{2+}-dependent K^+ conductance.

When K^+ currents are substantially blocked by inclusion of TEA in the bathing medium and internal perfusion of the cell with Cs^+ via the patch electrode, GH_3 cells exhibit inward current upon depolarization, due to Ca^{2+} entry (18, 24, 25). There is also residual outward current that could be due to the passage of Cs^+ ions through K^+ channels or other cation pores. The amplitude of the residual outward current is a small fraction of that observed under usual recording conditions. Nevertheless, as shown in Fig. 5C, this residual outward current can also be facilitated by 4-AP. Note that the peak inward current is slightly diminished during 4-AP administration, due to the facilitation of opposing outward currents. When outward currents are more completely blocked by intracellular and extracellular solutions containing NMG-Cl (see Materials and Methods), 4-AP has no effect on the sustained inward Ca^{2+} current and no longer promotes outward current (six cells). These results demonstrate that the aminopyridine facilitation of outward current does not result from an enhancement of Ca^{2+} entry through voltage-dependent Ca^{2+} channels.

Although all drug solutions were adjusted to physiological pH before use, control for pH artifacts was carried out by applying bathing medium that had been adjusted to pH 6.5 or 8.6. Neither of these solutions produced an effect on the sustained outward current similar to that of the aminopyridines.

Fig. 7 illustrates that aminopyridines promote the sustained outward current at all potentials at which the steady state current-voltage curve shows rectification, indicating that the current is activated (i.e., potentials more positive than −25 mV). 4-AP does not cause a modification in the current-voltage characteristics of the cell in the nonrectifying voltage region below −30 mV and does not shift the threshold for activation of the sustained outward current.

Fig. 8 illustrates the dose dependency of the effect of 4-AP and 3,4-DAP on the sustained outward current. At the highest concentrations, the drug produces more than a doubling in the steady state current amplitude. Lower concentrations produced less effect, in a dose-dependent fashion. At higher concentrations, 3,4-DAP appeared to be somewhat more potent than 4-AP, but this did not hold true at lower concentrations.

Characterization of the large-conductance Ca^{2+}-activated K^+ channel. Cell-attached single-channel recordings from GH_3 cells invariably demonstrated large-conductance Ca^{2+}-dependent K^+ channels. As illustrated by the recording shown in Fig. 9, these channels exhibited a marked voltage

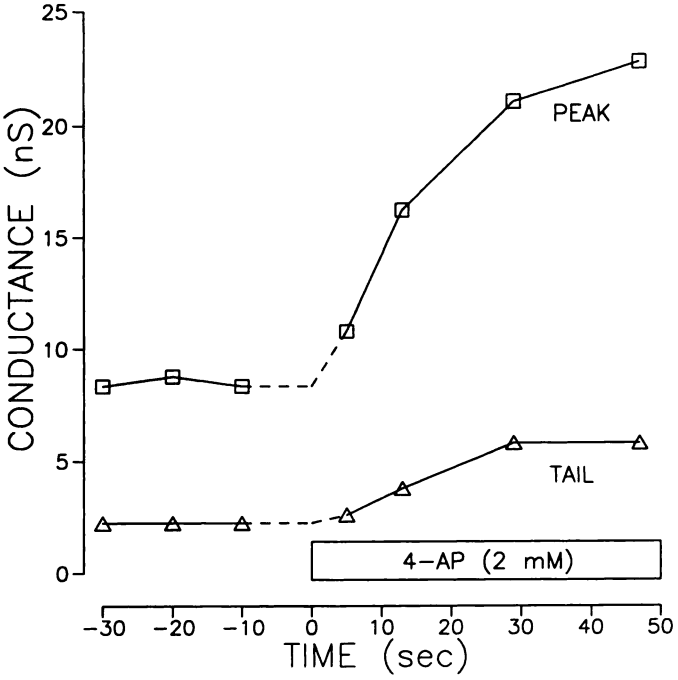

Fig. 6. Time course of the facilitation of sustained outward current by 4-AP. Five-second voltage steps from −50 to −10 mV were applied at intervals. After several control steps, superfusion with 2 mM 4-AP was begun (*bar*). The conductance for the maxinum outward current at the end of each step (*PEAK*) and for the corresponding tail current (*TAIL*) were determined as indicated in the legend to Fig. 3.

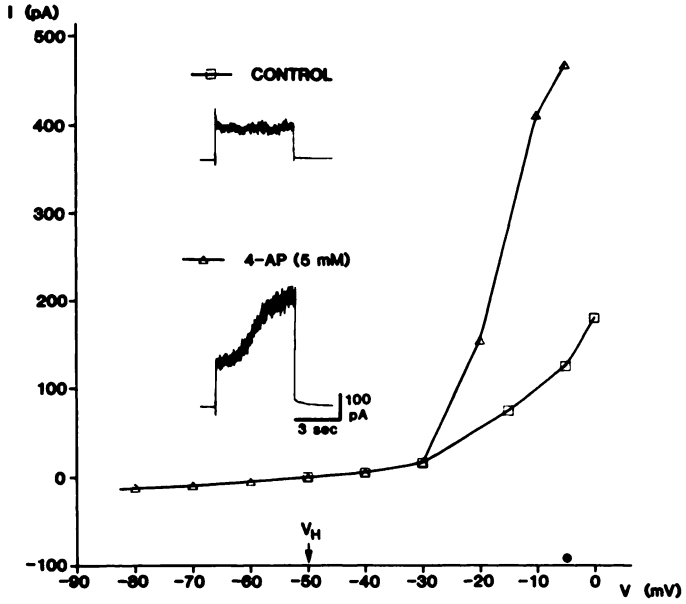

Fig. 7. Current-voltage relationship for sustained outward current before (□) and after (△) application of 4-AP (5 mM). The *points* represent the peak outward current obtained at the end of a 5-sec voltage clamp step from the holding potential (V_H, −50 mV) to the indicated command potentials. 4-AP does not alter the curve for step potentials below −30 mV. Above this level, the cell shows outward rectification and 4-AP increases the peak outward current. The *dot* indicates the step potential (−5 mV) for the *sample traces* in the *inset*.

dependency. Channel opening is infrequent at resting potential (0 mV electrode potential), but the open probability increases substantially with depolarization. Inspection of channel recordings of several minutes in duration indicated that the channels

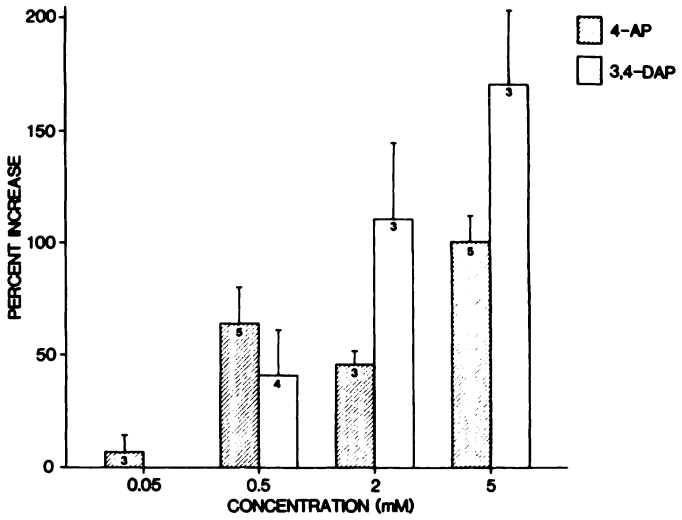

Fig. 8. Concentration dependency for the increase in sustained outward current produced by 4-AP and 3,4-DAP. The outward current was determined using voltage-clamp steps from −50 mV to between −25 and −10 mV. The control step amplitude was adjusted to give a moderate time-dependent rise in current during the voltage step. The percentage increase in peak outward current [$I_{K(Ca)}$] was calculated as $100 \times [I^*_{K(Ca)} - I_{K(Ca)}]/I_{K(Ca)}$ where $I_{K(Ca)}$ is the net outward current elicited by the voltage step at 5 sec and $I^*_{K(Ca)}$ is the maximum current measured in the same way during the drug application. The *bars* indicate the mean percentage increase; *numerals* indicate the number of cells tested; *lines* represent standard errors. The actual net current for the control steps was 231 ± 25 pA (mean ± SE).

did not inactivate with maintained depolarization. Single-channel records obtained in the cell-attached configuration often showed a slight sag (relaxation) in the open current. This sag was not present in excised patch recordings. The distortion presumably reflects loading of the open channel current by the cell capacitance under conditions in which the single-channel conductance is of significant magnitude in relation to the whole-cell conductance [see Fenwick *et al.* (26)]. In cell-attached recordings with 5.5 mM K^+ in the recording electrode, the mean channel amplitudes were linearly related to membrane potential (Fig. 10), giving single-channel conductances of 55–90 pS (mean ± SD: 67 ± 12, $n = 5$). With high K^+ in the recording electrode, the conductance increased to 150–175 pS (Fig. 10). In the present series of experiments, no attempt was made to study small-conductance Ca^{2+}-activated K^+ channels, as described by Lange and Ritchie (17).

Extracellular superfusion with TEA failed to affect the activity of Ca^{2+}-activated K^+ channels in cell-attached single-channel recordings, as expected if the drug is unable to permeate the cell membrane. However, in outside-out patch recordings, 20 mM TEA produced complete elimination of channel opening (Fig. 11), supporting the conclusion that the channels mediate the TEA-sensitive K^+ current activated by prolonged depolarization in these cells. Like TEA, external Cd^{2+} had no effect on channel openings in cell-attached patch recordings. This is as expected if Cd^{2+} inhibition of the sustained K^+ current in whole-cell recordings occurs as a result of Ca^{2+} entry blockade, because voltage-dependent Ca^{2+} channels are not activated during these recordings (except in the patch membrane itself and Cd^{2+} does not have access to these channels). To provide further support for this concept, the Ca^{2+} dependency of the channels were studied in single-channel recording experiments. As previously reported by Lange and Ritchie (17), the open

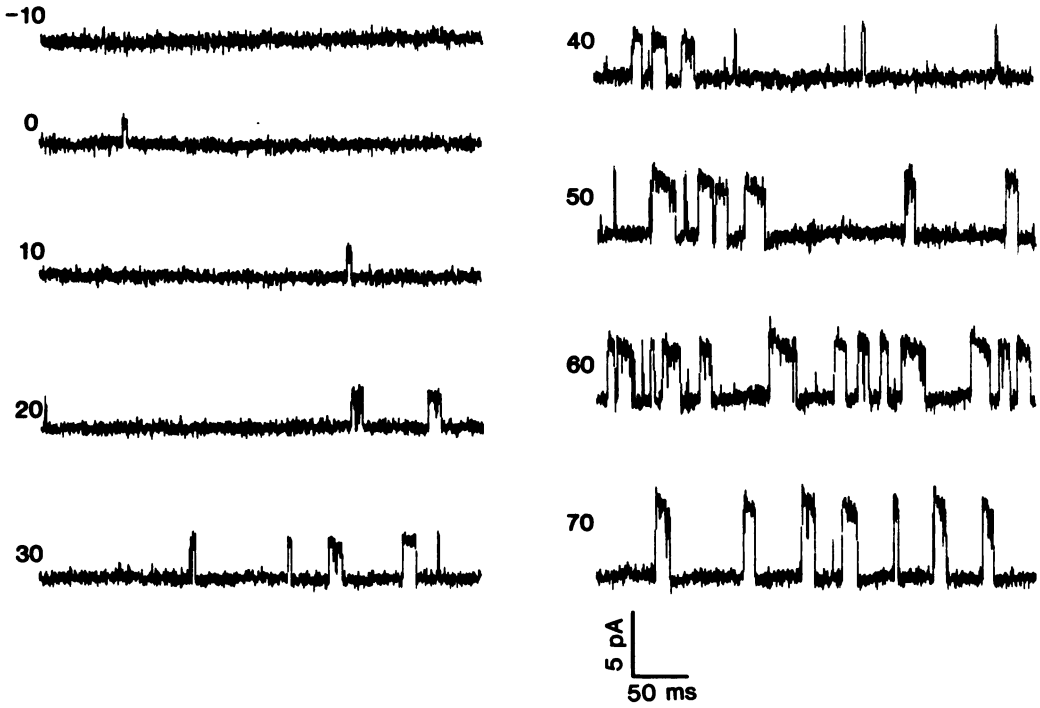

Fig. 9. Cell-attached patch recording of a single Ca^{2+}-activated K^+ channel with 5.5 mM K^+ in the electrode solution. *Numbers* to the *left* of each *record* reflect the relative depolarization of the patch with respect to the resting potential of the cell (negative of the patch electrode potential). Mean channel open times increased with depolarization from 2.6 (+10 mV) to 10.6 msec (+70 mV).

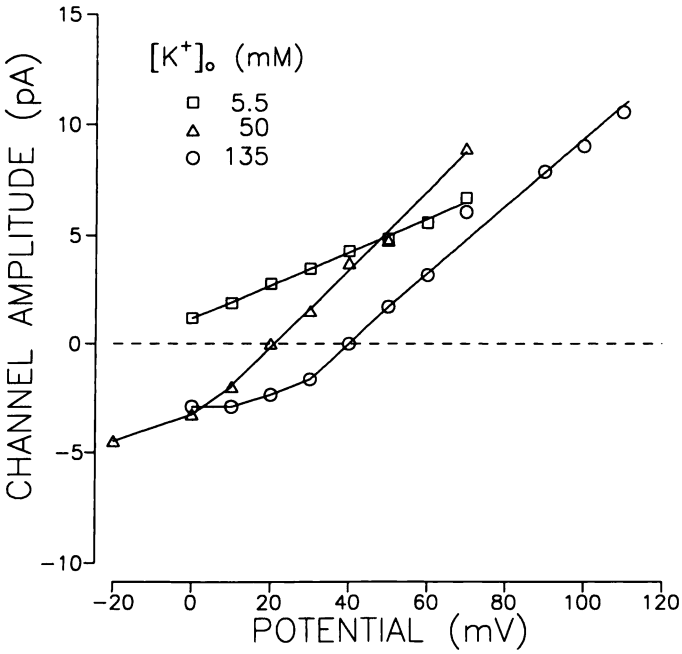

Fig. 10. Single-channel current-voltage relationships for three Ca^{2+}-activated K^+ channels in cell-attached patch recordings. Each recording was obtained with a different concentration of K^+ in the patch electrode solution, as indicated. The *points* represent the mean amplitudes of 101–455 discrete openings. When the open channel currents showed a sag (see text), the peak amplitudes were used. Individual amplitude values were normally distributed about the means with standard deviations <10% of the means. The data indicated by *squares* are from the channel illustrated in Fig. 9. Single-channel conductances, calculated from the best fit lines to the linear portions of the current-voltage plots, are as follows: 5.5 mM K^+, 75.9 pS; 50 mM K^+, 174 pS; 135 mM K^+, 152 pS. The reversal potentials for 50 and 135 mM KCl are 20 and 39 mV, respectively. The shift of 19 mV compares with a theoretical shift of 25 mV, indicating that the channels are predominantly, although perhaps not exclusively, permeable to K^+.

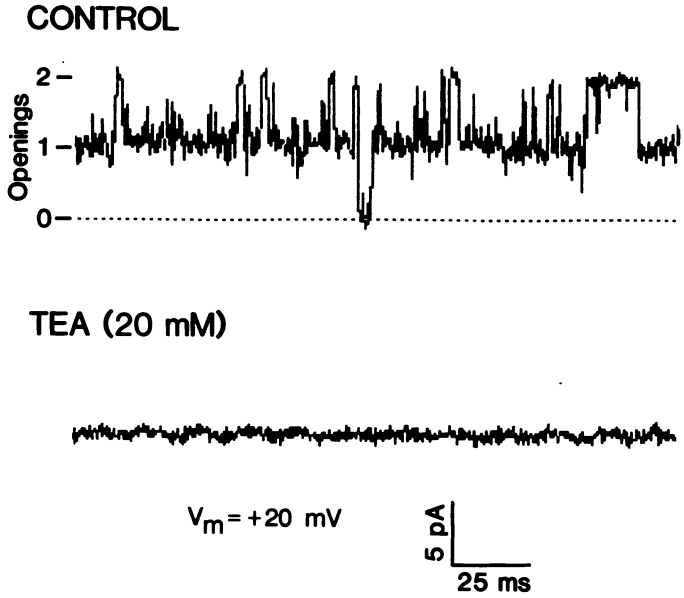

Fig. 11. Outside-out patch recording showing blockade of Ca^{2+}-activated K^+ channels by TEA (20 mM). Under control conditions at a holding potential of +20 mV, two channels were active in the patch. Superfusion with TEA results in the elimination of all openings. The pipette contained normal internal solution with nominally 4 μM free Ca^{2+} (1.1 mM EGTA, 1.08 mM $CaCl_2$); the bath contained normal bathing medium with 10 mM $CaCl_2$ and 2 mM $MgCl_2$. Holding potential (V_m), +20 mV. Single-channel conductance, 83 pS.

probability of large-conductance Ca^{2+}-activated K^+ channels in GH_3 cells was highly dependent upon the internal concentration of Ca^{2+}, with a threshold near 1 μM. In outside-out patch recordings at nominally 1 μM free internal Ca^{2+}, channel openings were observed only at strongly depolarized potentials (greater than +30 mV), whereas, with higher free Ca^{2+} concentrations (4–50 μM), the open probability was substantial at more hyperpolarized potentials. The Ca^{2+} dependency was confirmed in inside-out patch experiments in which the same

channel was perfused with bath solution containing different free Ca^{2+} concentrations. As illustrated in Fig. 12, the open probability at +40 mV is markedly increased upon transition from nominally 0.01 to 1 μM free Ca^{2+}. These results confirm the Ca^{2+} dependency of the large-conductance voltage-dependent K^+ channel and provide further evidence that it underlies the Cd^{2+}-sensitive outward current activated by long depolarization.

Facilitation of Ca^{2+}-activated K^+ channels by 4-AP. The mechanism of the aminopyridine facilitation of the sustained K^+ current was investigated by studying the effect of 4-AP on the single Ca^{2+}-dependent K^+ channels underlying the current. A typical cell-attached recording is illustrated in Fig. 13A. The patch membrane was depolarized 50 mV from resting potential so that the channels opened moderately frequently. Extracellular application of 4-AP (2 mM) led to a marked facilitation of channel opening within seconds of the onset of the drug perfusion. Whereas under control conditions simultaneous channel openings are rare, during and after 4-AP as many as three simultaneous openings were observed. The fraction of time spent in the open state was markedly enchanced by 4-AP (Fig. 13B); however, the drug did not significantly alter the single-channel conductance (Fig. 13C).

To further explore the mechanism of the 4-AP effect on single Ca^{2+}-activated K^+ channels, recordings were carried out in bathing medium nominally free of Ca^{2+}. Under these conditions, the channels did not open, even with strong depolarization (Fig. 14, *top left*). 4-AP failed to cause the appearance of channel openings in Ca^{2+}-free solution (Fig. 14, *bottom left*). However, in the same cell, extracellular application of Ca^{2+}-containing bathing solution resulted in channel opening and this was markedly facilitated by 4-AP. This suggests that the action of 4-AP is dependent upon sufficient intracellular Ca^{2+} to permit channel opening. The patch illustrated in the recording of Fig. 14 appears to contain only a single large-amplitude channel, as evidenced by the lack of simultaneous openings. This experiment, therefore, demonstrates that 4-AP can facilitate the activity of an individual Ca^{2+}-activated K^+ channel as well as possibly increase the number of active channels, as indicated by Fig. 13. In experiments with excised inside-out patches exposed to usual extracellular and intracellular Ca^{2+} concentrations (see Materials and Methods), 4-AP (5 mM) failed to have a direct effect on channel opening (n = 3), demonstrating that its facilitatory action requires intact cells.

Discussion

The main observation of this study is that aminopyridines can facilitate the sustained Ca^{2+}-activated K^+ current in intact GH_3 clonal pituitary cells. This is in sharp contrast to their blocking effect on voltage-dependent, Ca^{2+}-independent K^+ currents in GH_3 cells (15) and other cell types (see Introduction). The facilitatory effect is best observed with persistent depolarizations of at least several seconds and occurs at somewhat higher concentrations than the channel-blocking effects. Thus, the A-type K^+ current in GH_3 cells is substantially blocked by 4-AP concentrations in the micromolar range (15).

The Ca^{2+}-activated K^+ current is the dominant membrane current activated upon prolonged depolarization of GH_3 cells, and single-channel recordings consistently demonstrated large-conductance, noninactivating, Ca^{2+}- and voltage-dependent K^+ channels. The channels have unitary conductance with a physiological transmembrane K^+ gradient of 67 pS, but this increases to 150–175 pS in symmetrical high K^+. Although a similar unitary conductance for Ca^{2+}-activated K^+ channels was found in one previous study with GH_3 cells (27), Lang and Ritchie (17) have reported a conductance approximately double this value. The reason for the discrepancy is unclear but may relate to the use of cells derived from different GH_3 subclones. In fact, the unitary conductances of Ca^{2+}-activated K^+ channels varies widely in different tissues (28). Because of the possible variation in channel properties between cell preparations, it was important to characterize in detail the single-channel properties and pharmacological sensitivity of the channel as a prelude to examining the effects of 4-AP. These experiments demonstrated a Ca^{2+} dependency of the channel similar to that reported by Lang and Ritchie (17) and, in addition, showed the channel to be TEA sensitive. The results are consistent with the concept that the large-conductance Ca^{2+}-dependent K^+ channel is the primary carrier of the sustained K^+ current activated by prolonged depolarization.

The single-channel recordings provide insight into the way in which aminopyridines act to promote the sustained K^+

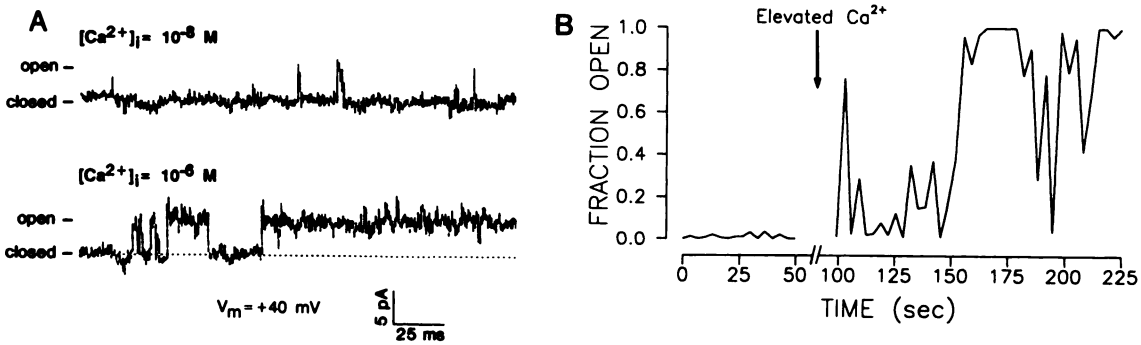

Fig. 12. Activity of a single Ca^{2+}-activated K^+ channel in an inside-out patch at two concentrations of internal free Ca^{2+}. The excised patch was initially made with the internal (cytoplasmic) membrane face exposed to nominally 10^{-8} M Ca^{2+}-containing medium (1.1 mM EGTA, 0.1 mM $CaCl_2$). The patch was continuously stepped at a rate of 0.3 Hz from −30 mV to +40 mV for a duration of 409 msec. (Potentials are with respect to the bath.) Sample records during the step are shown in A; small capacitative transients occurring at the onset of the step were eliminated by subtracting an averaged record composed of three blank sweeps. The graph shown in B plots the open probability of the channel during each sweep with respect to the time from the start of the experiment. During the break in the record (marked by an *arrow*), the bathing medium was changed to nominally 10^{-6} M Ca^{2+} (1.1 mM EGTA, 1 mM $CaCl_2$). There is a marked increase in the channel open probability with elevated Ca^{2+}. The conductance of the channel was 73 pS.

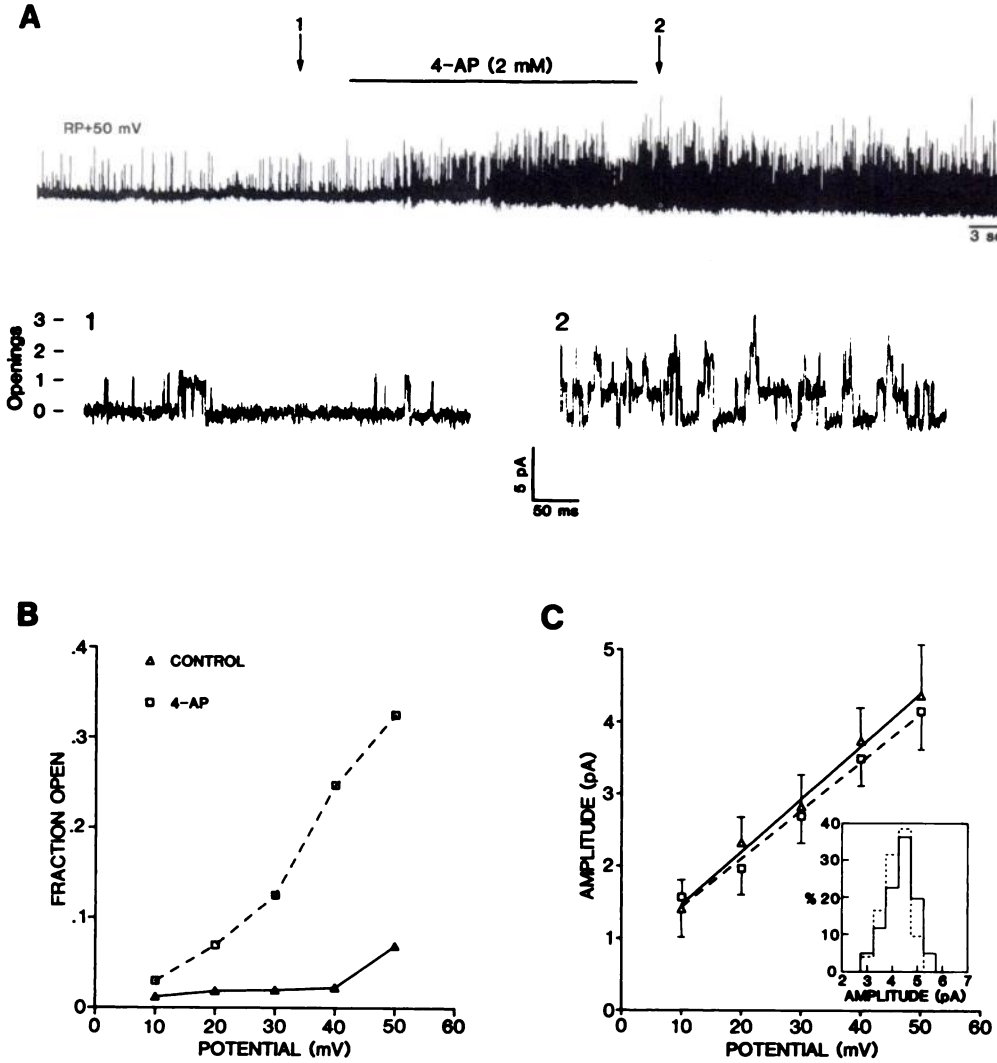

Fig. 13. Effect of 4-AP on single Ca^{2+}-activated K^+ channels in a cell-attached recording. All parts of the figure refer to the same experiment. A, *top*, the patch was depolarized by 50 mV. At this level of depolarization, channel openings occurred moderately frequently under control conditions. Superfusion of the cell with 4-AP (2 mM) greatly increased the frequency of channel opening. The pen recorder *tracing* does not give an accurate indication of the single-channel current amplitude due to its limited frequency response. *Bottom*, sample records (taken at *points* indicated by *arrows* in the *top tracing*) showing single channel currents on an expanded time scale. At least three channels were present in this patch. B, Effect of 4-AP on the fraction of time (*ordinate*) at least one channel is open at various potentials depolarized from resting potential (*abscissa*). Each *point* represents data (73–102 open events) obtained from continuous recording before (△) and during (□) 4-AP application. C, Single-channel amplitudes as a function of the depolarization potential. Each *point* represents the mean amplitude of the open events used in B; *bars* indicate standard deviation. At each potential level, the channel amplitude data exhibited a unimodal distribution, as indicated by the sample histograms for the data at 50 mV shown in the *inset* (——, control; – – –, 4-AP), demonstrating that all channels in this recording are of similar conductance. This suggests that 4-AP does not activate a distinct population of channels that are not open under control conditions. The least squares best fit line to the data gives a single-channel conductance of 73 pS for control (——) and 67 pS for 4-AP (– – –). These values are not significantly different by the small sample *t* test for parallelism (45).

current. In intact GH_3 cells, the drugs markedly enhance the open probability of the channel without altering their unitary conductance. Because the drugs have no effect on the channels in excised membrane patches, the drugs presumably do not act on the channels themselves and, in fact, the effect of aminopyridines is similar to that produced by increases in the intracellular free Ca^{2+} level. Nevertheless, the cellular mechanisms responsible for the facilitatory effect of aminopyridines on channel opening are a matter of speculation. In several systems, it has been suggested that 4-AP facilitates Ca^{2+} entry through voltage-sensitive Ca^{2+} channels (29–31). Such an action could potentially account for the effect on the Ca^{2+}-activated K^+ current and, in fact, the aminopyridines failed to promote the macroscopic current or the underlying single channels in Ca^{2+}-free bathing medium. However, effects on Ca^{2+} entry do not seem to explain the potentiation, because 4-AP did not promote Ca^{2+} current in GH_3 cells (Fig. 5C). Bathing GH_3 cells in Ca^{2+}-free medium lowers intracellular Ca^{2+} levels (32–35) and because the channels require Ca^{2+} for their activation, this would result in their failure to open and does not imply an extracellular Ca^{2+} requirement specifically for the aminopyridine effect. The single-channel recordings also provide evidence against a specific effect on Ca^{2+} current, because in these experiments the whole cell was not depolarized to a potential level at which voltage-dependent Ca^{2+} channels are activated (24, 25). Moreover, depolarization of the patch tends to hyperpolarize the whole cell slightly so that Ca^{2+} currents are even less likely to become activated. 4-AP is known to cause increased spike firing

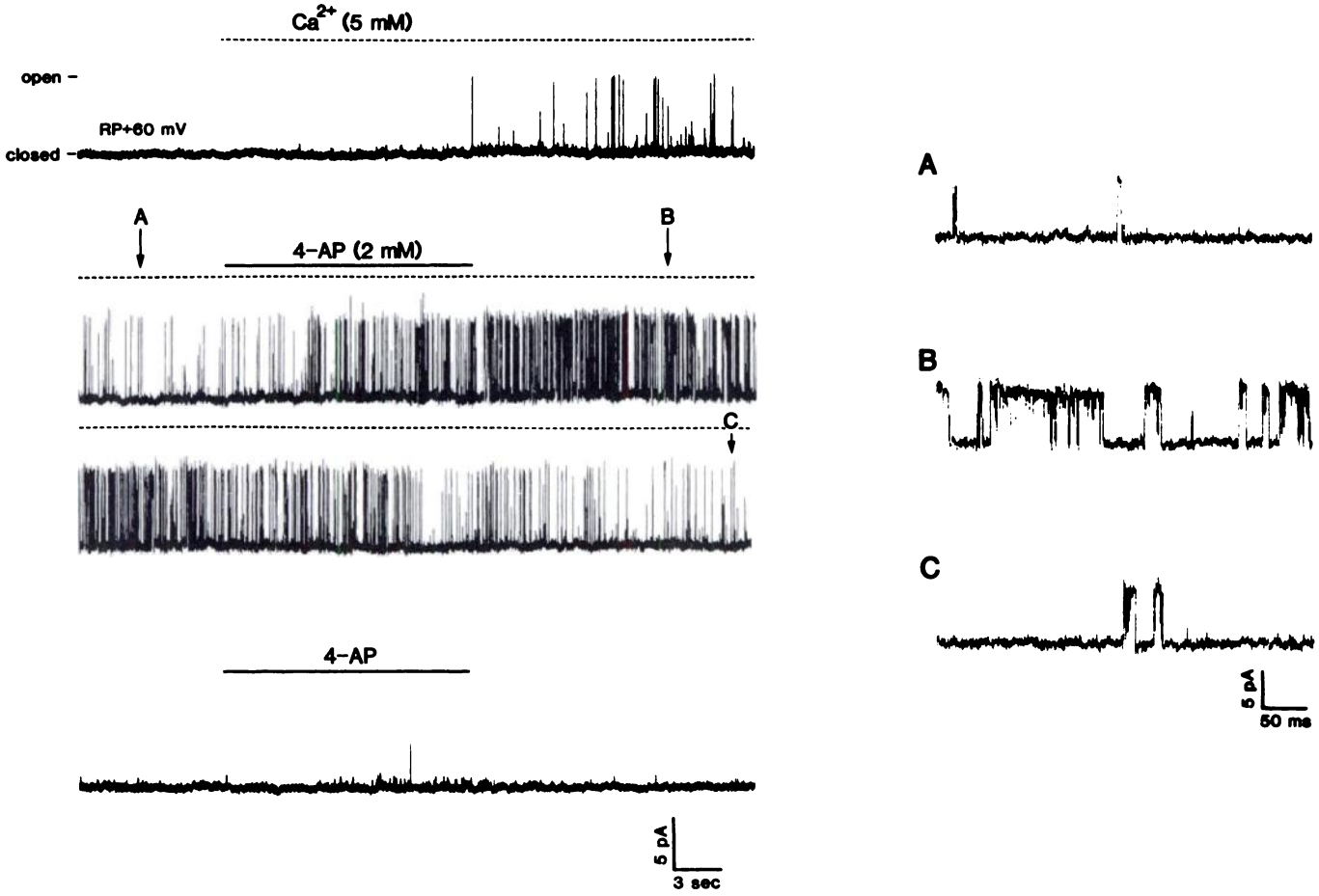

Fig. 14. Failure of 4-AP to promote single Ca^{2+}-activated K^+ channels in Ca^{2+}-free solution. This cell-attached recording was carried out with nominally Ca^{2+}-free extracellular and pipette solution. Under these conditions, large amplitude channel openings are not observed (*top left*). When the cell is exposed to Ca^{2+}-containing recording medium (applied during period indicated by *dashed line*) channel opening is permitted and this activity is enhanced by 4-AP (applied during period indicated by *solid line*). The *middle two traces* form a continuous record. Segments of this record displayed on an expanded time base are shown to the *right*; the *letters* indicate the approximate point at which the fast sweeps were taken. *Bottom left trace* indicates lack of effect of 4-AP under Ca^{2+}-free conditions. This patch contained a channel of conductance 90 pS; an unidentified small amplitude channel may be present as well.

in GH_3 cells (2). However, when the patch electrode is held at −50 or −60 mV (Figs. 13 and 14), the cell is sufficiently hyperpolarized so that there are no spontaneous action potentials, even in the presence of 4-AP.[1] Therefore, the increased spike firing and resulting Ca^{2+} entry that usually occurs with 4-AP cannot account for the effect on Ca^{2+}-activated K^+ channels. Additional evidence against the concept that the aminopyridine effect is mediated by a facilitation of Ca^{2+} entry was obtained previously by Herman and Gorman (10). These investigators reported that high concentrations of 4-AP (5 mM) increased the Ca^{2+}-activated K^+ current in a molluscan pacemaker neuron. In these experiments, Ca^{2+} was injected intracellularly by iontophoresis so that possible effects on Ca^{2+} current were excluded.

As an alternative hypothesis, it can be speculated that the aminopyridines interfere with the Ca^{2+}-handling ability of the cell, so that intracellular Ca^{2+} levels effectively rise and shift the activation curve for the Ca^{2+}-dependent channels to more hyperpolarized levels. Thus, Ca^{2+}-activated K^+ channels were not promoted in excised patches, where cellular Ca^{2+}-buffering mechanisms are absent. Moreover, the delayed nature of the 4-AP effect could be due to a gradual overwhelming, during a prolonged voltage step, of the Ca^{2+}-buffering capacity either in the whole cell or in a localized compartment within the cell. Additional evidence in favor of this idea is provided by experiments carried out in Na^+-free extracellular medium (NMG-MSA bath solution). 4-AP produced a much larger increase in outward current under these conditions than in normal Na^+-containing medium. In excitable cells, the Ca^{2+} gradient is maintained by a Na^+-Ca^{2+} exchange mechanism (36). Recent studies have demonstrated the existence of Na^+-Ca^{2+} exchange in plasma membrane vesicles from GH_3 cells (37). In the absence of extracellular Na^+, this exchange process is inhibited and Ca^{2+} cannot be discharged from the cell. Thus, if aminopyridines impaired Ca^{2+} buffering or transport, intracellular Ca^{2+} would rise more rapidly and achieve a higher level in Na^+-free conditions.

Alterations in cytoplasmic pH could also contribute to the aminopyridine effect. 4-AP and 3,4-DAP are strongly basic compounds, with pK_a values of 9.17 and 9.14, respectively (38). It has recently been demonstrated that elevation of intracellular pH increases the activity of Ca^{2+}-activated K^+ channels in

[1] Unpublished observations.

pancreatic β-cells (39, 40) and epithelial cells (41, 42). Like the facilitation occurring in GH_3 cells, this is the result of an increase in the open channel probability (41). It has been proposed that H^+ can compete with Ca^{2+} for binding to the Ca^{2+} regulatory site on the channel. Thus, elevation of intracellular pH would relieve the H^+ block and produce an action effectively similar to an increase in intracellular free Ca^{2+}. Assuming this mechanism, the greater maximum efficacy of 3,4-DAP, compared with 4-AP (Fig. 8), would result from the presence of two basic groups on the molecule.

4-AP has been demonstrated to promote prolactin release from GH_3 cells (2). Hormone release from these cells is stimulated by increases in intracellular Ca^{2+} levels (32, 43, 44). If 4-AP enhances the effective intracellular free Ca^{2+} concentration, this could account for the effect of the drug on release, apart from any stimulation of action potential firing.

Acknowledgments

The author wishes to thank Dr. Jeffery L. Barker, in whose laboratory these experiments were begun, and Dr. Stephen A. George for his assistance with the experiment shown in Fig. 12.

References

1. Thesleff, S. Aminopyridines and synaptic transmission. *Neuroscience* **5**:1413–1419 (1980).
2. Sand, O., E. Harug, and K. M. Gautvik. Effects of thyroliberin and 4-aminopyridine on action potentials and prolactin release and synthesis in rat pituitary cells in culture. *Acta Physiol. Scand.* **108**:247–252 (1980).
3. Pelhate, M., and Y. Pichon. Selective inhibition of potassium current in the giant axon of the cockroach. *J. Physiol (Lond.)* **242**:90–91P (1974).
4. Yeh, J. Z., G. S. Oxford, C. H. Wu, and T. Narahashi. Interaction of aminopyridines with potassium channels of squid axon membranes. *Biophys. J.* **16**:77–81 (1976).
5. Meeves, H., and Y. Pichon. The effect of internal and external 4-aminopyridine on the potassium currents in intracellularly perfused giant axons. *J. Physiol. (Lond.)* **268**:511–532 (1977).
6. Fink, R., and E. Wettwer. Modified K-channel gating by exhaustion and the block by internally applied TEA^+ and 4-aminopyridine in muscle. *Pflügers Arch. Eur. J. Physiol.* **374**:289–291 (1978).
7. Molgó, J. Voltage-clamp analysis of the sodium and potassium currents in skeletal muscle fibers treated with 4-aminopyridine. *Experientia (Basel)* **34**:1275–1276 (1978).
8. Thompson, S. H. Three pharmacologically distinct potassium channels in molluscan neurones. *J. Physiol. (Lond.)* **265**:465–488 (1977).
9. Rogawski, M. A. The A-current: how ubiquitous a feature of excitable cells is it? *Trends Neurosci.* **5**:214–219 (1985).
10. Herman, A., and A. L. F. Gorman. Effects of 4-aminopyridine on potassium currents in a molluscan neuron. *J. Gen. Physiol.* **78**:63–86 (1981).
11. Barker, J. L., B. Dufy, D. G. Owen, and M. Segal. Excitable membrane properties of cultured central nervous system neurons and clonal pituitary cells. *Cold Spring Harbor Symp. Quant. Biol.* **48**:259–268 (1983).
12. Dubinsky, J. M., and G. S. Oxford. Ionic currents in two strains of rat anterior pituitary tumor cells. *J. Gen. Physiol.* **83**:309–339 (1984).
13. Barros, F., G. J. Kaczorowski, G. M. Katz, R. L. Vandlen, and J. P. Reuben. Application of whole-cell voltage clamp in the study of neuroendocrine cells, in *Electrophysiological Techniques in Pharmacology* (H. M. Geller, ed.). Alan R. Liss, Inc., New York, 149–168 (1986).
14. Ritchie, A. K. Two distinct calcium-activated potassium currents in a rat anterior pituitary cell line. *J. Physiol. (Lond.)* **385**:591–609 (1987).
15. Rogawski, M. A. Transient outward current (I_A) in clonal anterior pituitary cells: blockade by aminopyridine analogs. *Naunyn-Schmiedeberg's Arch. Pharmacol.* **338**:125–132 (1988).
16. Pappone, P. A., and M. T. Lucero. *Pandinus imperator* scorpion venom blocks voltage-gated potassium channels in GH_3 cells. *J. Gen. Physiol.* **91**:817–833 (1988).
17. Lang, D. G., and A. K. Ritchie. Large and small conductance calcium-activated potassium channels in the GH_3 anterior pituitary cell line. *Pflügers Arch. Eur. J. Physiol.* **410**:614–622 (1987).
18. Rogawski, M. A., K. Inoue, S. Suzuki, and J. L. Barker. A slow calcium-dependent chloride conductance in clonal anterior pituitary cells. *J. Neurophysiol.* **59**:1854–1870 (1988).
19. Blatz, A. L., and K. L. Magelby. Ion conductance and selectivity of single calcium-activated potassium channels in cultured rat muscle. *J. Gen. Physiol.* **84**:1–23 (1984).
20. Smart, T. G. Single calcium-activated potassium channels recorded from cultured rat sympathetic neurones. *J. Physiol. (Lond.)* **389**:337–360 (1987).
21. Benham, C. D., T. B. Bolton, R. J. Lang, and T. Takewaki. The mechanism of action of Ba^{2+} and TEA on single Ca^{2+}-activated K^+-channels in arterial and intestinal smooth muscle membranes. *Pflügers Arch. Eur. J. Physiol.* **403**:120–127 (1985).
22. Wong, B. S., and M. Adler. Tetraethylammonium blockade of calcium-activated potassium channels in clonal anterior pituitary cells. *Pflügers Arch. Eur. J. Physiol.* **407**:279–284 (1986).
23. Simasko, S. M., G. A. Weiland, and R. E. Oswald. Pharmacological characterization of two calcium currents in GH_3 cells. *Am. J. Physiol.* **254**:E328–E336 (1988).
24. Hagiwara, S., and H. Ohmori. Studies of calcium channels in rat clonal pituitary cells with patch electrode voltage clamp. *J. Physiol. (Lond.)* **331**:231–252 (1982).
25. Matteson, D. R., and C. M. Armstrong. Na and Ca channels in a transformed line of anterior pituitary cells. *J. Gen. Physiol.* **83**:371–394 (1984).
26. Fenwick, E. M., A. Marty, and E. Neher. A patch-clamp study of bovine chromaffin cells and of their sensitivity to acetylcholine. *J. Physiol. (Lond.)* **331**:577–597 (1982).
27. Dubinsky, J. M., and G. S. Oxford. Dual modulation of K channels by thyrotropin-releasing hormone in clonal pituitary cells. *Proc. Natl. Acad. Sci. USA* **82**:4282–4286 (1985).
28. Petersen, O. H., and Y. Maruyama. Calcium-activated potassium channels and their role in secretion. *Nature (Lond.)* **307**:693–696 (1984).
29. Lundh, H. Effects of 4-aminopyridine on neuromuscular transmission. *Brain Res.* **153**:307–318 (1978).
30. Illes, P., and S. Thesleff. 4-Aminopyridine and evoked transmitter release from motor nerve endings. *Br. J. Pharmacol.* **64**:623–629 (1978).
31. Rogawski, M. A., and J. L. Barker. Effects of 4-aminopyridine on calcium action potentials and calcium current under voltage clamp in spinal neurons. *Brain Res.* **280**:180–185 (1983).
32. Moriarty, C. M., and M. P. Leuschen. Role of calcium in acute stimulated release of prolactin from neoplastic GH3 cells. *Am. J. Physiol.* **240**:E705–E711 (1981).
33. Leuschen, M. P., C. M. Moriarty, and H. W. Sampson. Calcium movements and intracellular calcium distribution in neoplastic GH3 cells. *Histochemistry* **77**:85–97 (1983).
34. Schlegel, W., and C. B. Wollheim. Thyrotropin-releasing hormone increases cytosolic free Ca^{2+} in clonal pituitary cells (GH_3 cells): direct evidence for the mobilization of cellular calcium. *J. Cell Biol.* **99**:83–87 (1984).
35. Gershengorn, M. C., and C. Thaw. Thyrotropin-releasing hormone (TRH) stimulates biphasic elevation of cytoplasmic free calcium in GH_3 cells: further evidence that TRH mobilizes cellular and extarcellular Ca^{2+}. *Endocrinology* **116**:591–596 (1985).
36. Baker, P. F. Transport and metabolism of calcium ions in nerve. *Prog. Biophys. Mol. Biol.* **24**:177–223 (1972).
37. Kaczorowski, G. J., L. Costello, J. Dethmers, M. J. Trumble, and R. L. Vandlen. Mechanisms of Ca^{2+} transport in plasma membrane vesicles prepared from cultured pituitary cells. I. Characterization of Na^+/Ca^{2+} exchange activity. *J. Biol. Chem.* **259**:9395–9403 (1984).
38. Barlin, G. B. Ionization constants of heterocyclic substances. VI. Some substituted pyridines. *J. Chem. Soc.* 1201–2280 (1964).
39. Cook, D. L., M. Ikeuchi, and W. Y. Fujimoto. Lowering of pH_i inhibits Ca^{2+}-activated K^+ channels in pancreatic B-cells. *Nature (Lond.)* **311**:269–271 (1984).
40. Rosario, L. M., and E. Rojas. Modulation of K^+ conductance by intracellular pH in pancreatic *beta*-cells. *FEBS Lett.* **200**:203–209 (1986).
41. Christensen, O., and T. Zeuthen. Maxi K^+ channels in leaky epithelia are regulated by intracellular Ca^{2+}, pH and membrane potential. *Pflügers Arch. Eur. J. Physiol.* **408**:249–259 (1987).
42. Hunter, M., K. Kawahara, and G. Giebisch. Calcium-activated epithelial potassium channels. *Miner. Electrolyte Metab.* **14**:48–57 (1988).
43. Ronning, S. A., and T. F. J. Martin. Characterization of Ca^{2+}-stimulated secretion in permeable GH_3 pituitary cells. *J. Biol. Chem.* **261**:7834–7849 (1986).
44. Gershengorn, M. C. Mechanism of thyrotropin releasing hormone stimulation of pituitary hormone secretion. *Annu. Rev. Physiol.* **48**:512–526 (1986).
45. Kleinbaum, D. G., and L. L. Kupper. *Applied Regression Analysis and Other Multivariate Methods.* Duxbury Press, North Scituate, MA (1978).

Send reprint requests to: Michael A. Rogawski, M.D., Ph.D., Medical Neurology Branch, NINDS, NIH, Building 10, Room 5N-248, Bethesda, MD 20892.